On the role of orifice wetting for Al and Al22.5wt%Cu with Al_2O_3 in the Discharge Crucible method

R.S.P. Flood and H. Henein
Dept. of Chemical and Materials Engineering
University of Alberta
Edmonton, Alberta

Abstract

The demand to develop Materials Genomics and Integrated Materials Computation requires the availability of high temperature property data of liquid metals. As computing power and algorithms are constantly being improved, the accuracy of thermophysical property data has emerged as one of the limiting factors. Knowledge of these properties for materials such as Al and Al-alloys is a critical factor in numerical simulations and modelling of a wide array of industrial processes. This work reports on the measurement of viscosity, surface tension and density of liquid Al and Al-22.5wt.%Cu using the Discharge Crucible method. By comparing to other experimental data published in literature, as well as several theoretical and empirical models, the results from this study have achieved, with a varying degree of success, the goal of validating the Discharge Crucible method as a viable, cost-effective measurement method. However, while viscosity and surface tension proved to be in good agreement with other published data and model calculations, density were found to be significantly lower than expected. Through analysis, it was determined that wetting of Al or Al-Cu at the orifice of the Al_2O_3 crucible has an effect on flow rate since modelling of the flow using the modified-Bernoulli formulation does not account for accelerative losses within the meniscus. Dimensionless number analysis identified that wetting had an immediate effect on the flow rate, becoming more dominant with decreasing Capillary number, and hence drain time. In looking at the sensitivity of the Discharge Crucible model, it was determined that density had the largest effect on flow rate, thus explaining the link between the role of orifice wetting and the inaccurate density measurements (as opposed to viscosity or surface tension). Future research will aim to extend the Discharge Crucible model and method to account for wetting at the orifice, particularly at high temperatures.

1. Introduction

Aluminum is roughly a third of the weight of steel, which makes it particularly suitable for the automotive and aerospace industries. It is also used in the building, electrical, machinery, consumer durables, and packaging industries. It has high corrosion resistance, conductivity, impermeability, and strength, and is aesthetic, relatively inexpensive to produce, and essentially infinitely recyclable. One billion tonnes of Al has been produced since 1886, and three quarters of that metal is still in use [1]. Al and its alloys are generally first melted and then undergo different forming processes, such as casting, continuous casting, pressure die casting, metal injection molding, and additive manufacturing. In current practices, computer-based simulations enable the modelling of the casting, melting and remelting processes, as well as heat transport, solidification, shrinkage, residual stresses and welding [2]. Thermophysical properties are critical inputs for these simulation models. For example, viscosity is required to model convection and macro-segregation during solidification [3]. Surface tension is vital to the castability and mold filling ability of the metal or alloy [4], and also for modelling surface tension driven flow, i.e. the Marangoni effect, during welding [5]. And, density is a fundamental property often required to quantify other properties using theoretical or semi-empirical models.

These data are typically very difficult and time consuming to measure, and thus, there would be great benefit to industry if a complete database of these properties existed. This information would not only facilitate modelling for process optimization, but also the development of new, improved multi-component alloys. Industrial stakeholders are keen to develop this database, as more data could help them create alloys quicker, cheaper and with more environmental sustainability. Historically, there are wide discrepancies in the thermophysical property data reported in literature. For example, there is a spread of roughly 400% in the reported values for Al viscosity [6]. These discrepancies are mainly attributed to the nature of materials becoming highly reactive at high temperatures. Contamination is persistently an issue, and although there are a wide array of measurement methods to pick from, most fall victim to the same limitations. This is especially detrimental when measuring both viscosity and surface tension of Al-based liquids, as contamination, particularly with oxygen, has proven to drastically affect the values measured using conventional techniques. As computers and models continue to improve, the accuracy of the thermophysical property measurements has become one of the limiting factors.

In recent years, the levitated drop method using electromagnetic levitation (EML) has become increasingly popular in measuring the viscosity, surface tension and density of metallic liquids. It has the advantage of being a containerless method which significantly reduces sources of contamination. It is also able to simultaneously measure multiple properties at once. However, the levitated drop method has a few important drawbacks, such as the inability to measure viscosity terrestrially, evaporation of volatile elements, and poor control of oxygen partial pressure. To address the first limitation, an EML apparatus was installed on the International Space Station. Not surprisingly, this has a significant effect on the cost of each property measurement.

One, terrestrial-based, alternative to using the EML for the simultaneous measurement of viscosity, surface tension and density of metallic liquids is the Discharge Crucible (DC) method. The DC method, developed by Roach and Henein [7] at the University of Alberta, is a ground-based technique able to simultaneously measure the surface tension, viscosity and density of

metallic liquids in a simple, robust and cost-effective manner. The DC method is based on the Bernoulli formulation which describes the fluid dynamics of an inviscid liquid draining from a crucible through an orifice under the influence of gravity, forming a free jet. The rate of liquid flow is proportional to the head of the liquid inside the crucible. It is assumed that the flow at the top of the crucible and the exit of the orifice is in quasi-steady state, i.e. no acceleration effects, the velocity at the top of the crucible is much less than at the exit of the orifice, and that pressures at the inlet of the crucible and at the exit of the orifice are atmospheric. The detailed derivation of the model is described elsewhere [8]. The formulation modified to account for viscous losses is given as:

$$Q_{exp} = C_d \pi r_o^2 \sqrt{2g\left(h - \frac{\sigma}{\rho g r_o}\right)} \tag{1}$$

Where Q_{exp} is the actual (experimental) flow rate of the liquid draining from the crucible, and C_d is the discharge coefficient, which describes the viscous losses within the crucible and orifice, and is a function of the Reynolds number, Re. The height of the fluid in the crucible is given by h, g is the gravitational acceleration, ρ and σ are the density and surface tension, respectively, and r_o is the radius of the orifice in the crucible.

When conducting experiments, h and Q_{exp} change with time, while all other variables are constant, with the exception of C_d. A specific experimental setup (i.e. unique crucible geometry, orifice size) can be calibrated by generating a general C_d versus Re function using a liquid with known properties, where $Re = 2\rho Q_{exp}/\pi r_o^2 \eta$, and η is viscosity. This function is assumed valid for liquids having different thermophysical properties, since it solely dependent on the geometry of the crucible and orifice.

As such, if the C_d versus Re function is, for example, linear, i.e. $C_d = a(Re) + b$, Eq. 1 can be written as:

$$Q_{exp} = \left(a\left(\frac{2\rho r_o Q_{exp}}{\pi r_o^2 \eta}\right) + b\right) \pi r_o^2 \sqrt{2g\left(h - \frac{\sigma}{\rho g r_o}\right)} \tag{2}$$

Eq. 2 is the basis on which measurements are carried out, and effectively models the flow of the liquid draining from the crucible under the influence of gravity.

For measurements of liquids with unknown properties, a calibrated setup is used. η, σ and ρ are simultaneously calculated using a non-linear least squares regression. The computation uses a Gauss-Newton algorithm to minimize the errors, or residuals, $r_i(\beta)$, from a series of datapoints, h and Q_{exp}, acquired from a single high-temperature experiment:

$$r_i(\beta) = h_{i,exp} - f\left(Q_{i,exp}, \beta\right) \tag{3}$$

Where variables β and model function $f\left(Q_{i,exp}, \beta\right)$ are defined as:

$$\beta = \begin{bmatrix} \sigma \\ \eta \\ \rho \end{bmatrix} \tag{4}$$

$$f(Q_{i,exp},\beta) = \frac{1}{2g}\left(\frac{Q_{i,exp}}{C_d \pi r_o^2}\right)^2 + \frac{\sigma}{\rho g r_o} \quad (5)$$

The model function, $f(Q_{i,exp},\beta)$, is written by re-arranging Eq. 2 and isolating head, h. A more detailed description of the formulation and computation of the DC method is outlined elsewhere [8].

The DC method has been used to successfully measure the surface tension, viscosity and density of various pure low and high melting temperature liquids, like water, ethylene glycol, Al, Pb, Sb, Ga, and Zn [9]–[12]. It has also been used to determine the thermophysical properties of various alloys, such as Al-Mg, Al-Zn, Al-Mg-Zn, Sb-Sn-Zn, Sb-Sn, Ga-Zn, Ga-Sn, Ga-Sn-Zn and Pb-Sb [9], [10], [13]–[15]. There was initial skepticism with regards to low reported viscosity value (e.g. approximately 50% lower than values obtained in literature) for measurements on pure liquid Al, however, this was later attributed to high O content in the atmosphere [11]. A recent study repeated the experiments on Al, and reported viscosity values that aligned much closer to literature values [9].

In this work, the DC method will be used to measure the thermophysical properties of pure liquid Al and an Al-Cu alloy. Previous work conducted using the DC method have relied on the use of crucible materials resistant to wetting, such as graphite or Teflon. However, for higher melting-point liquids, like Fe and steel, which require crucibles with incredibly low reactivity and high heat-resistance, wetting may become problematic. Roach and Henein [7] cautioned: "If wetting is an issue, the liquid may spread along the orifice exit effectively altering the radius of the exiting stream". The DC model assumes a constant radius and a cylindrical exit stream; therefore, wetting would likely cause discrepancies in accurately predicting flow, resulting in measurement errors. Thus, this study seeks to investigate the effect of wetting on the DC method. This will be achieved by using a high-purity Al_2O_3 crucible, a material more susceptible to wetting by both Al and Al-Cu.

1. Experimental

In this study, measurements were conducted on two different samples: pure Al and an Al-Cu alloy, comprised of 22.5 wt.% Cu. The samples were prepared using 99.99 wt.% Al and 99.99 wt.% Cu shots. The experimental apparatus consisted of two main sections: the furnace unit and the collection unit, shown in Fig. 1. The furnace unit is comprised of a 20kW power supply, water-cooled induction coils, graphite susceptor, a high-purity Al_2O_3 crucible, and thermocouple to record melt temperature. The Al_2O_3 crucible had a 5.3 mm chamfered hole drilled through the bottom to allow the melt to drain. An Al_2O_3 stopper rod was designed to plug the orifice until the melt reached the desired temperature.

To avoid O contamination, the apparatus was cyclically purged using a vacuum pump, and filled with inert Ar to a gauge pressure of 34.5 kPag (5 psig), with the O_2 content continuously monitored using a ZrO_2 analyzer. A Ti-sponge getter was installed inside the apparatus; it reduces the O_2 content from 10 ppm to roughly 10^{-9} ppm.

The collection unit consisted of a steel container, filled with SiO_2 for heat dissipation. It is bolted on top of a s-beam load cell. At the desired temperature for measurement, the stopper rod

was removed, and the melt allowed to drain into the steel container. The load cell measures and records the collected mass of the draining liquid as a function of time. This data was then used to calculate volumetric flow rate and head of the draining Al or Al-Cu, which was subsequently used to compute viscosity, surface tension and density of the liquid at the specific temperature .

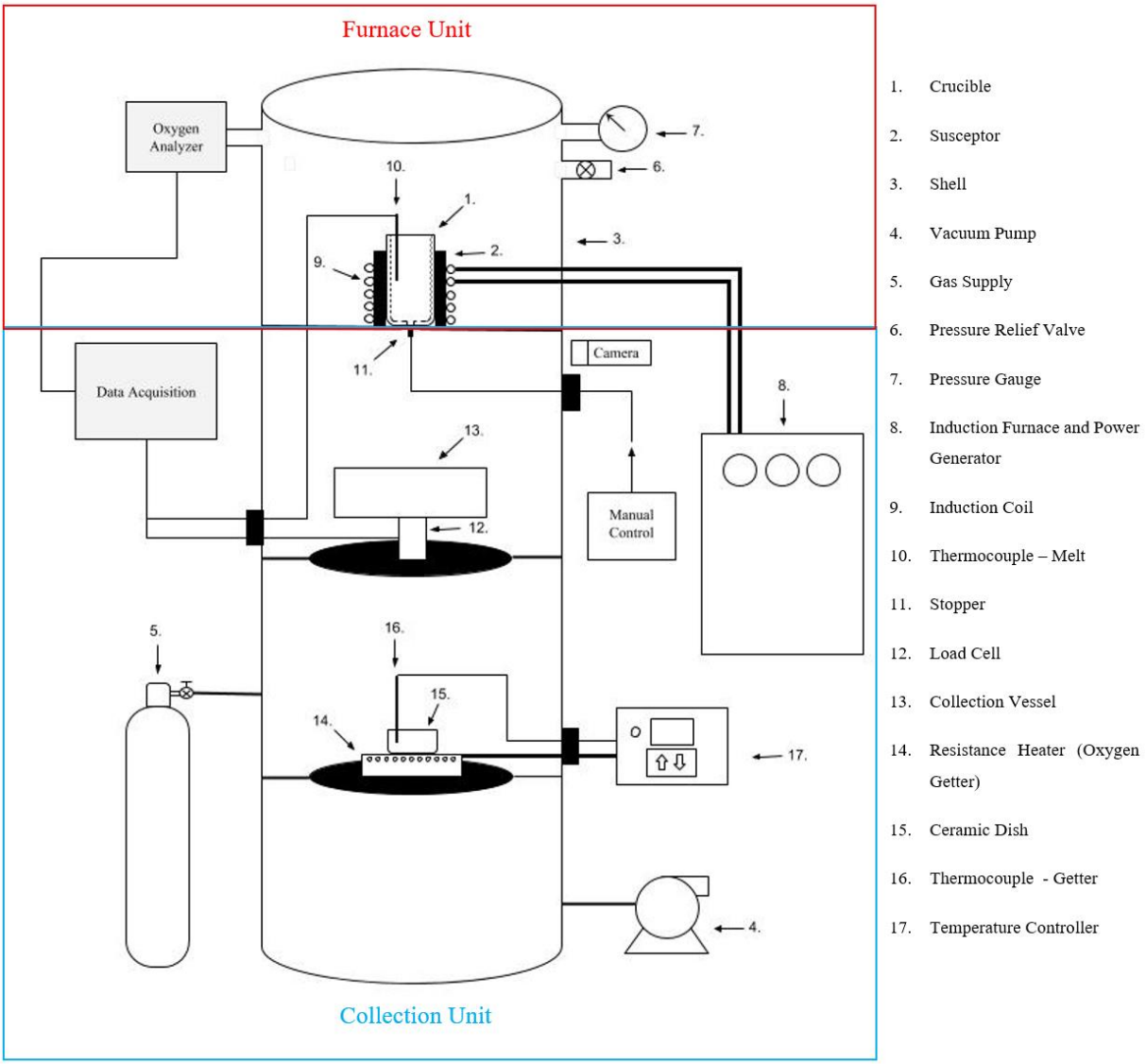

Figure 1: Schematic of high-temperature discharge crucible apparatus

Each high-temperature experiment was performed using a unique single-use crucible; therefore, separate calibrations were required. The C_d versus Re functions were obtained using deionized water at 298 K. Four individual experiments (see Fig. 2) were performed for each calibration and the data was averaged by fitting to a 3rd order polynomial. During calibration, it was observed that water gradually wets the base of the Al_2O_3 crucible as it exits orifice. Thus, prior to calibrating, the base of the crucibles were sprayed with a hydrophobic coating.

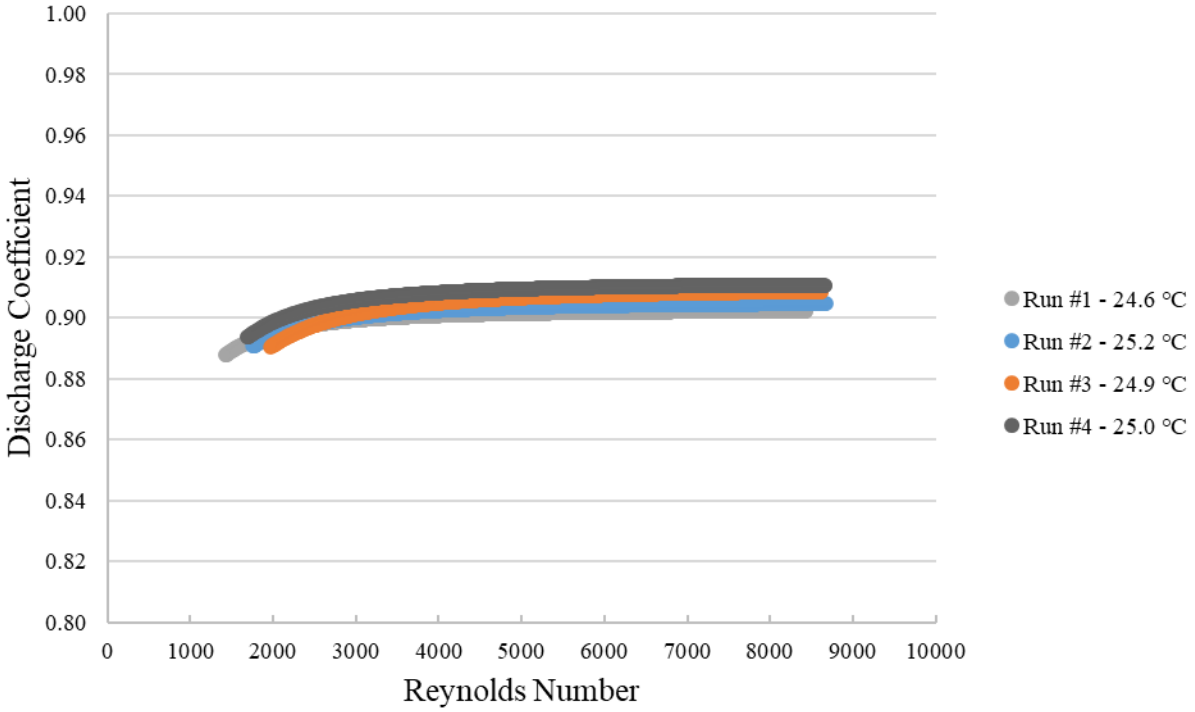

Figure 2: C_d versus Re calibration with deionized water of Al_2O_3 crucible used for measurement of Al at 1032 K

The experimental flow rate, Q_{exp}, of Al and Al-Cu was determined by curve fitting the load cell data (mass versus time). First, the raw data was trimmed, tared, and smoothed using a Savitzky-Golay filter. Then, the data was fitted to a 2nd order polynomial curve (see Fig.3), and mass flow rate was calculated by taking the 1st order derivative of the polynomial. Finally, the mass flow rate was converted to volumetric flow rate, Q_{exp}, by dividing by the density of the melt. The density was estimated from the literature for liquid Al and Al-Cu [6], [16].

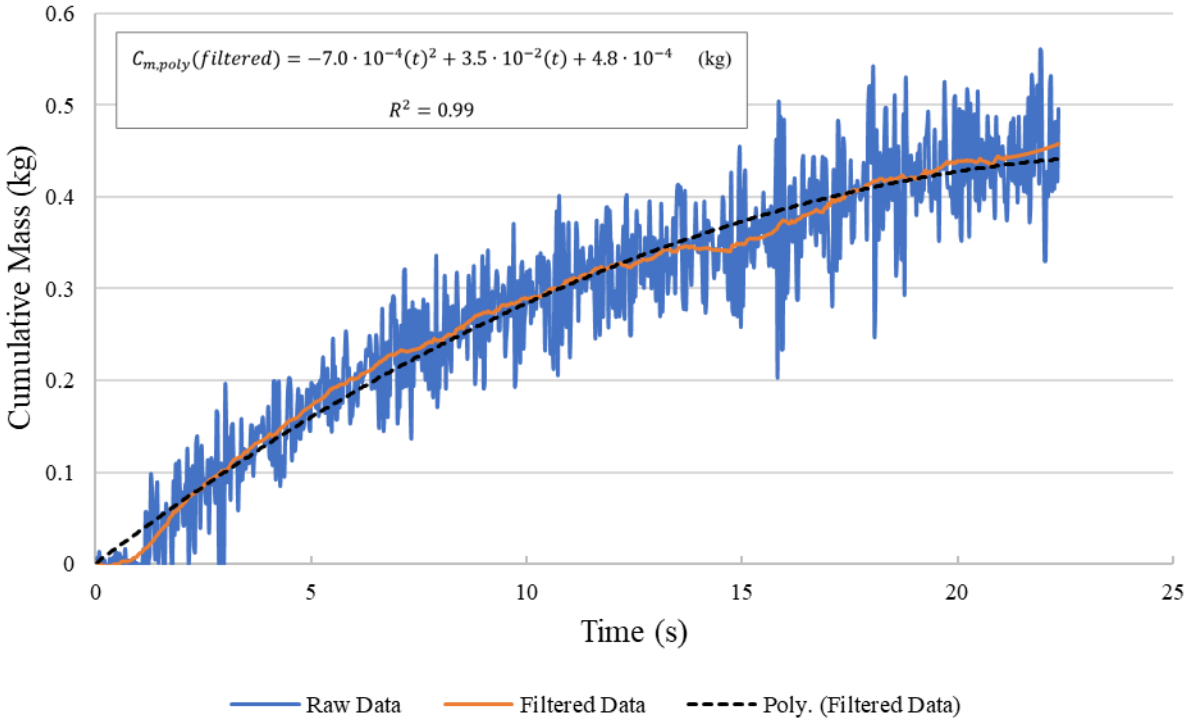

Figure 3: Cumulative mass of Al at 1032 K with fitted polynomial to raw data and filtered data

The head height, h, of Al and Al-Cu was determined by relating the volume of the liquid inside the crucible to a height calibration curve obtained using an ultrasonic level sensor. The ultrasonic level sensor was used to directly measure head of the water in the Al_2O_3 at various volumes. This curve was then used to determine the decreasing head of Al and Al-Cu as the liquid drained, by calculating the volume remaining in the crucible as a function of time. The volume remaining in the crucible was calculated using the load cell mass data divided by the estimated density of the liquid from literature, similar to how volumetric flow rate was calculated.

2. Results and Discussion

In running a multiple nonlinear regression using MATLAB, the viscosity, surface tension and density of Al and Al-Cu were determined at different measured temperatures. Experiments on pure Al were performed at 1032, 1120 and 1174 K, and on Al-Cu at 1029, 1076, 1123, 1180 and 1174 K. The measurements for surface tension, viscosity and density of Al and Al-Cu are presented in Table 1. In addition, the minimum measured O_2 content, initial charge mass, and start and end heads are also all shown in the Table 1. The radii of each orifice were determined prior to beginning the experiment and all measured 2.65 mm.

Table 1: Viscosity, surface tension and density of Al and Al-Cu determined experimentally at various temperatures using the DC method

Melt Material	Mass (kg)	Temperature (K)	O_2 Content (ppm)	Start Head (cm)	End Head (cm)	Viscosity (Pa·s)	Surface Tension (N/m)	Density (kg/m^3)
Al	0.568	1032	$1x10^{-8}$	8.45	2.25	$1.07x10^{-3}$	0.881	1588
Al	0.600	1120	$4x10^{-10}$	8.31	1.87	$8.62x10^{-4}$	0.859	1994
Al	0.544	1174	$2x10^{-9}$	8.24	1.98	$1.10x10^{-3}$	0.847	1804
Al-Cu	0.665	1029	$3x10^{-9}$	8.12	1.47	$1.66x10^{-3}$	0.877	2357
Al-Cu	0.600	1076	$1x10^{-9}$	7.32	1.55	$1.64x10^{-3}$	0.867	2433
Al-Cu	0.600	1123	$2x10^{-9}$	7.37	1.71	$9.32x10^{-4}$	0.842	2121
Al-Cu	0.671	1180	$8x10^{-10}$	8.14	1.84	$9.66x10^{-4}$	0.824	2133
Al-Cu	0.586	1224	$4x10^{-10}$	7.57	1.40	$7.24x10^{-4}$	0.808	2529

The results for Al and Al-Cu in Table 1 were compared with literature data obtained using a variety of measurement methods, including oscillating vessel, gas-bubble viscometry, sessile drop, levitated drop, maximum bubble pressure, drop weight, x-ray attenuation and pulse heating [3], [7], [23]–[32], [9], [33]–[37], [16]–[22] . There are a multitude of sources containing data for pure Al, however, most measurements describe an O saturated liquid. To avoid oxide contamination in liquid Al, an O partial pressure of 10^{-50} atm is required [38]. This is nearly impossible to achieve experimentally. Conversely, for Al-Cu (22.5 wt.% Cu), no literature sources exist for direct comparison with that exact composition. Nevertheless, experiments were conducted on very similar alloys containing 20 wt.% and 21 wt.% Cu, which more or less possess similar properties. To facilitate comparison between experimental results from this study, and those reported in literature, the combined data from literature were elaborated by a simple linear regression performed using the Fit Regression Model in Minitab 19 Statistical Software. This analysis proved useful in understanding the spread in data reported in literature by calculating standard errors (SE) and the 95% prediction intervals (PI), as well as understanding the consistency between results obtained in this study and previous studies reported in literature. Note, viscosity data was fitted to a linearized Arrhenius equation.

SE represents the average distance that the observed values fall from the regression line. It is calculated from the mean square error (MSE) of the regression:

$$\mathrm{SE} = \sqrt{MSE} \tag{6}$$

$$\mathrm{MSE} = \frac{\sum\left(Y_i - \widehat{Y}_i\right)^2}{(N - P - 1)} \tag{7}$$

Y_i is the i[th] observed response value, $\widehat{Y}_i$ is the i[th] fitted response, N is the number of observations, and P is the number of coefficients in the model, not including the constant.

PI defines the range that is likely to contain the response value of a single new observation given specified settings of the predictors in the regression model. The 95% PI is calculated as follows:

$$\widehat{Y}_0 = t_{(1-\alpha/1,\ N-P)} \cdot \sqrt{MSE}(1 + \boldsymbol{X_0'}(\boldsymbol{X'X})^{-1}\boldsymbol{X_0}) \tag{8}$$

Where $\widehat{Y}_0$ is the fitted response value for a given set of predictor values, t is the t-score, α is the level of significant (0.05 for 95% PI), $\boldsymbol{X}$ is the predictor matrix, and $\boldsymbol{X_0}$ is the matrix of given predictor values.

Al and Al-Cu viscosity measurements were plotted alongside comparable viscosity data (similar composition) published in literature in Fig. 4 and Fig. 5, respectively. The regression equation parameters were used to plot the best-fit Arrhenius curve for the combined literature data, as well as the plus and minus SE bounds and the 95% PI, as shown in Fig. 4 and Fig. 5, with the summarized regression output given in Table 2.

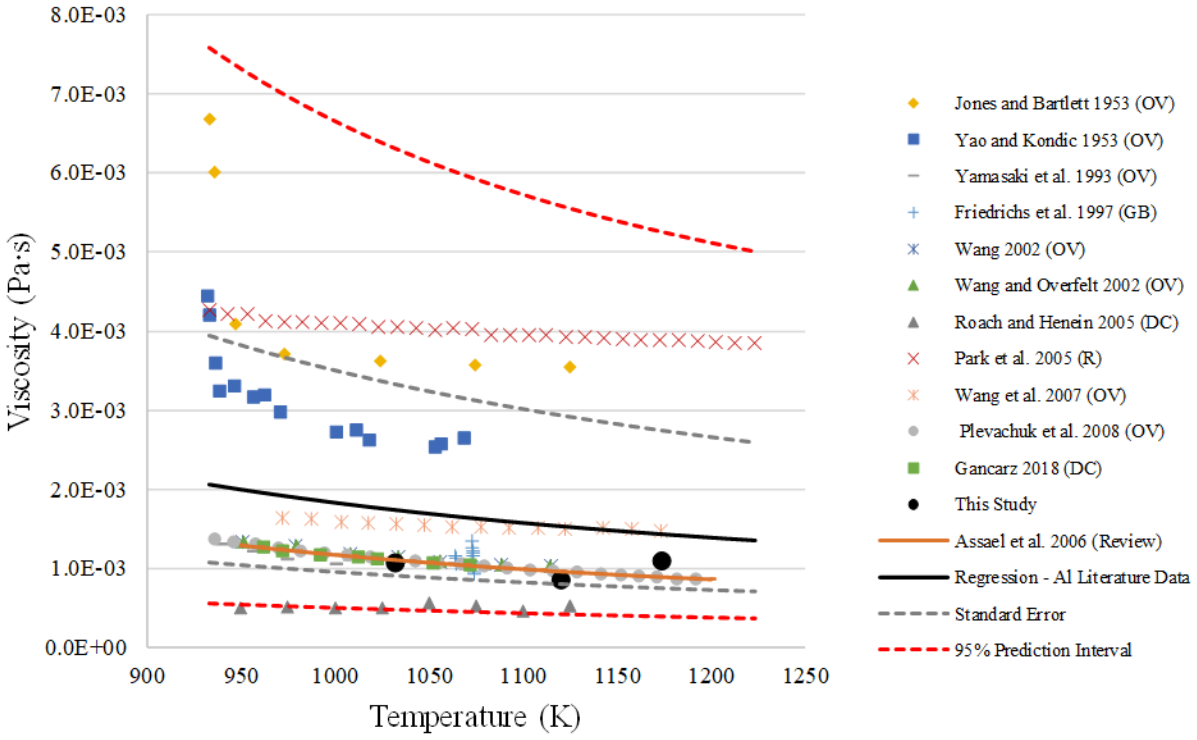

Figure 4: Comparison of Al viscosity measured using the DC method and data published in literature

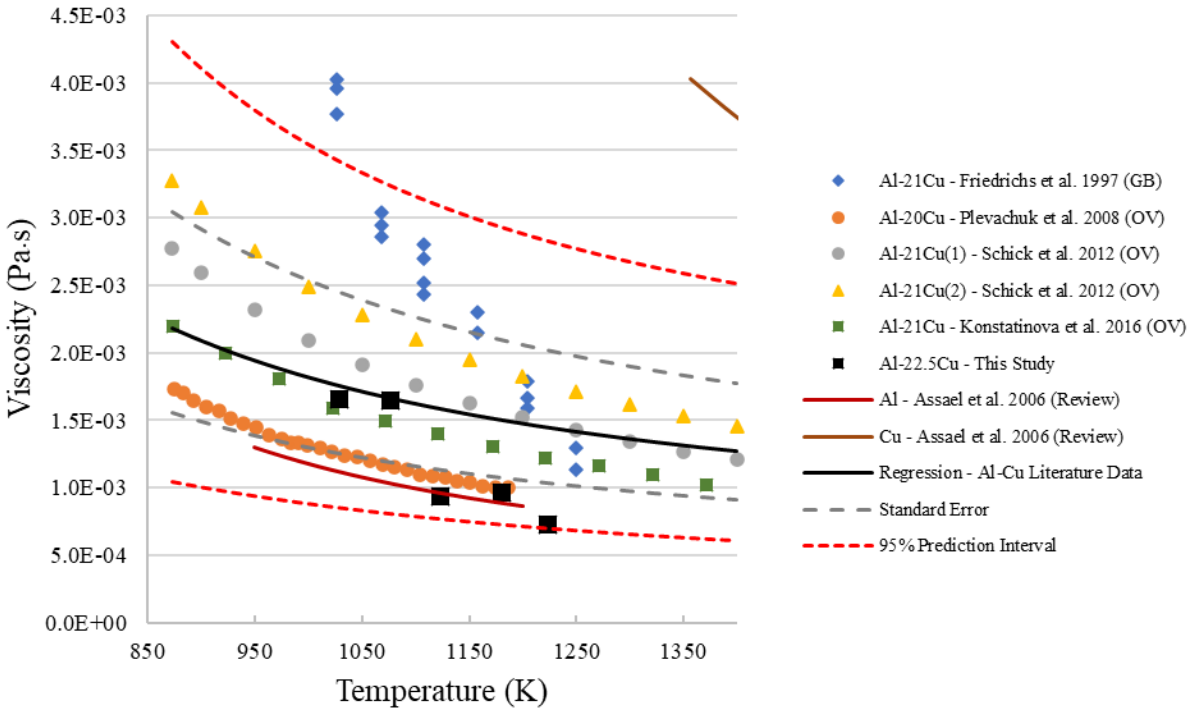

Figure 5: Comparison of Al-Cu viscosity measured using the DC method and data published in literature

Table 2: The coefficients of linearized Arrhenius equations in relation to the temperature dependence of viscosity for Al and Al-Cu experimental results and collected literature data

Melt Materials	$\ln\eta = \ln\eta_\infty + \frac{E_a}{RT}$ (ln[Pa·s])				
	N	Temp. Range (K)	$\ln\eta_\infty$ ln(Pa·s)	E_a (J)	SE ln(Pa·s)
Al Literature Data	139	933 – 1225	-7.96	13700	0.65
Al	3	1032 – 1174	-7.10	1810	0.19
Al-Cu Literature Data	81	873 – 1400	-7.56	10400	0.33
Al-Cu	5	1029 – 1224	-11.73	46000	0.16

The Al and Al-Cu results measured using the DC method all lie within the 95% PI of the literature data regression model, indicating good agreement with literature. Furthermore, the Al results are in even better agreement with comparable literature data, with all measurements falling within plus or minus one SE. The Al measurements agree particularly well with values reported by Gancarz *et al.* [9], Plevachuk *et al.*[16], Wang [39], and Yamasaki *et al.* [19], and suggested values by Assael *et al.* [6]. Not all Al-Cu viscosity measurements fall within plus or minus one SE. There is considerable scatter between data obtained by different researchers (as indicated by the large 95% PI), highlighting that the viscosity data for Al-Cu alloys published in literature is limited, and often contradictory.

The above-mentioned scatter between different studies in literature may be caused by challenges associated with melt contamination at high temperatures. Researchers have shown that superficial oxide films affect the measured viscosity of Al and Al alloys [40]. Furthermore, for DC experiments, solid oxide particles may form and can be trapped between the liquid and the orifice, drastically affecting the flow profile, and therefore the viscosity [41]. Dinsdale [40] suggests that the viscosity of Al decreases as the purity of the metal increases, due to various experimental factors, like the choice of crucible material. All of these observations are supported by experiments revealing that the apparent viscosity of Al increases as the oxygen content in the atmosphere increases [6]. This is validated in Fig. 4, where very early studies (i.e. 1950s, by Jones and Bartlett [17] and Yao and Kondic [18]) reported much higher Al viscosity measurements; highlighting recent technological advancements with regards to O_2 control, metal purity and experimental design.

The Al and Al-Cu surface tension results were plotted alongside comparable data published in literature and the regression fit of the combined literature data (including SE bounds and 95% PI). This is shown in Fig. 6 and Fig. 7 for Al and Al-Cu, respectively. The summarized outputs of the regression analysis are provided in Table 3. The surface tension measurements reported in literature are in excellent agreement with each other; the SE for all Al literature data is 3.99×10^{-2} N/m (N=179), which is equivalent to 5% error at T_m, and is 5.95×10^{-2} (N=96) for Al-Cu, equivalent to 7% at T_m. This highlights the consistency of surface tension measurements between various researchers and measurement methods.

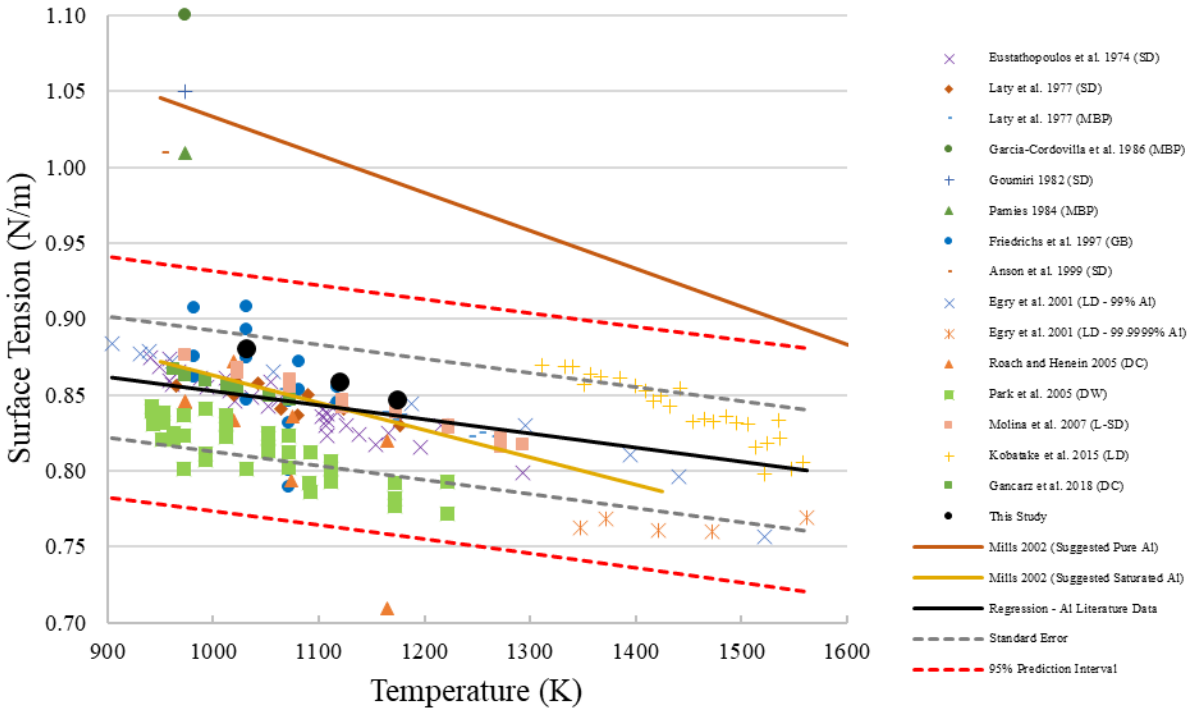

Figure 6: Comparison of Al surface tension measured using the DC method and data published in literature

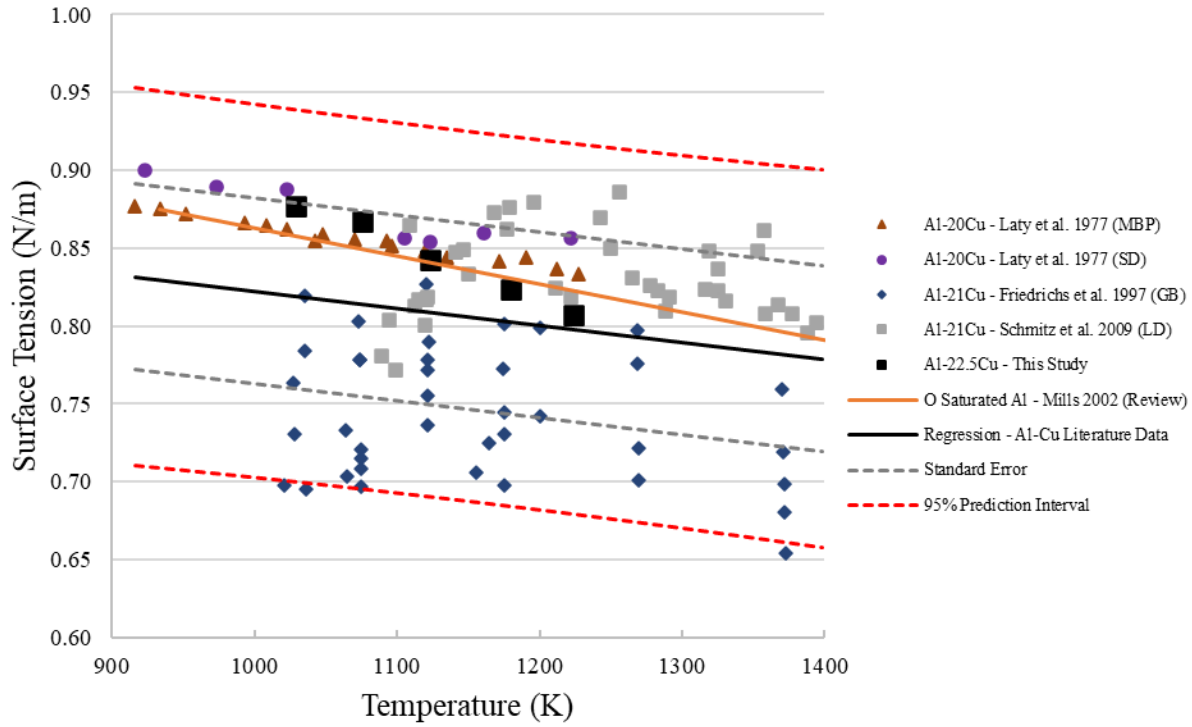

Figure 7: Comparison of Al-Cu surface tension measured using the DC method and data published in literature

Table 3: The coefficients of linear temperature dependance of surface tension for Al and Al-Cu experimental results and collected literature data

Melt Material	$\sigma_t = \sigma_m + \frac{d\sigma}{dT}(T - T_m)$ (N/m)					
	N	Temp. Range (K)	T_m (K)	σ_m (N/m)	$\frac{d\sigma}{dT}$ (N/m·K)	SE (N/m)
Al Literature Data	179	900 – 1560	933	0.859	-9.26×10^{-5}	3.99×10^{-2}
Al	3	1032 – 1174	933	0.904	-2.39×10^{-4}	6.01×10^{-4}
Al-Cu Literature Data	96	915 – 1500	867	0.837	-1.09×10^{-4}	5.95×10^{-2}
Al-Cu	5	1029 – 1224	867	0.940	-3.70×10^{-4}	3.57×10^{-3}

Mills [36] reported a confidence level 2% across four separate surface tension datasets which were used to calculate suggested values provided for O saturated Al. In considering results measured at 1032, 1120 and 1174 K, the difference between Mills and this study are no greater than 3%. Garcia-Cordovilla [42], Goumiri [43], Anson *et al.* [38] and Pamies [37] all took extraordinary measures to determine the surface tension of effectively pure Al, or non O saturated Al. These results, as shown in Fig. 6 are all much higher in magnitude. There is good consistency between Al-Cu results from this study and results obtained using EML-LD (Schmitz *et al.* [44]), SD (Laty *et al.* [26]) and MBP (Laty *et al.* [26]). As shown in Fig. 7 the surface tension of Al-rich Al-Cu is very similar to pure O saturated Al. To reduce the energy at the surface, Al will segregate to the surface since it has a lower surface tension than Cu. Moreover, O will also absorb to the surface, further reducing surface tension. Consequently, the surface tension for Al-rich Al-Cu alloys are only marginally larger than the surface tension of O saturated Al.

The density measurements determined in this study as well as results published in literature are shown in Fig. 8 and Fig. 9 for Al and Al-Cu, respectively, along with the fitted regression models and the 95% PI and SE intervals. The regression outputs are provided in Table 4.

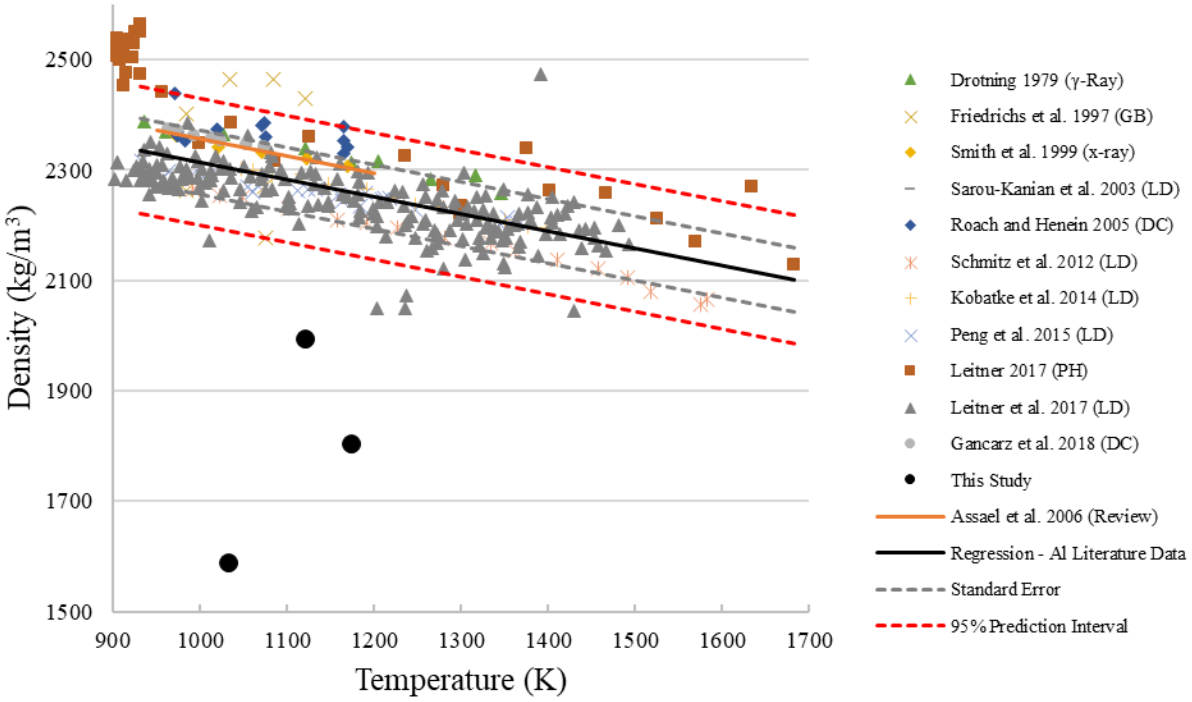

Figure 8: Comparison of Al density measured using the DC method and data published in literature

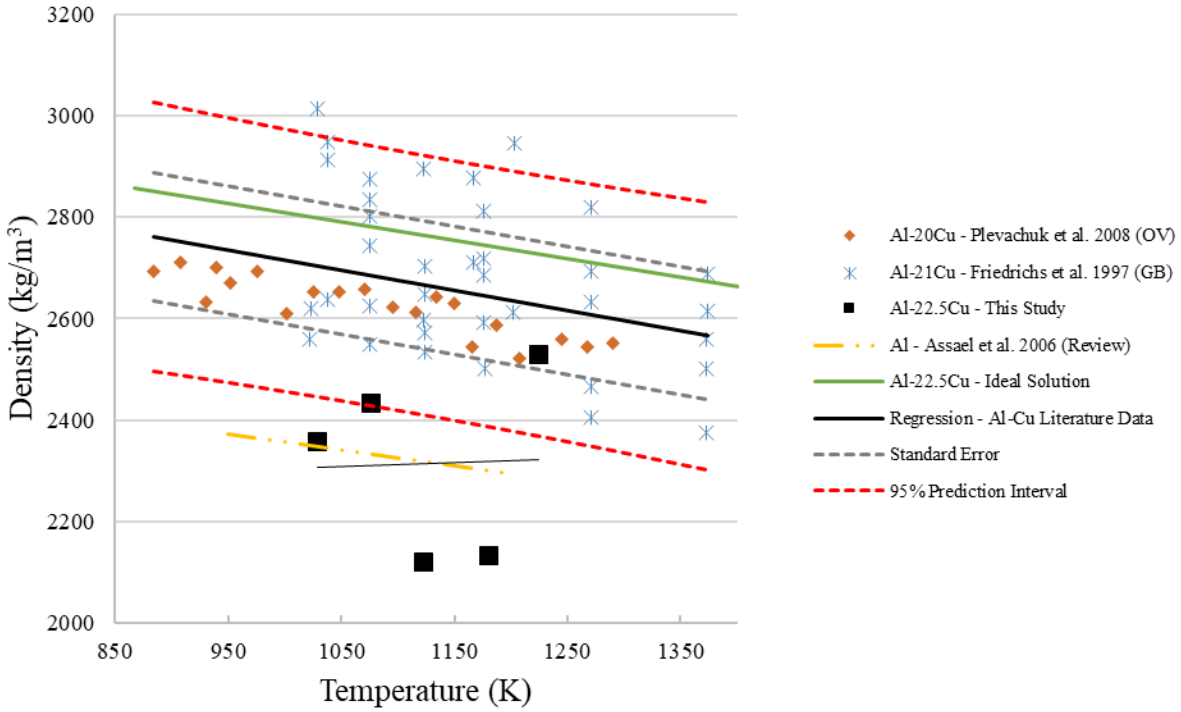

Figure 9: Comparison of Al-Cu density measured using the DC method and data published in literature

Table 4: The coefficients of linear temperature dependance of density for Al and Al-Cu experimental results and collected literature data

Melt Material	$\rho = \rho_m + \frac{d\rho}{dT}(T - T_m)$ (kg/m^3)					
	N	Temp. Range (K)	T_m (K)	ρ_m (kg/m^3)	$\frac{d\rho}{dT}$ (kg/m^3·K)	SE (kg/m^3)
Al Literature Data	293	930 – 1680	933	2335	-0.31	58
Al	3	1032 – 1174	933	1474	1.83	220
Al-Cu Literature Data	58	885 – 1375	867	2769	-0.40	126
Al-Cu	5	1029 – 1224	867	2296	0.07	210

The densities measured in this study are significantly lower than data reported in literature, falling well outside plus or minus one SE of the literature data regression models. Further, all Al results lie outside the 95% PI, and three of five Al-Cu measurements as well. The slopes for both the measured Al and Al-Cu as a function of temperature are also, incorrectly, positive. The density values published in literature for both Al and Al-Cu are in excellent agreement across various studies; whereas density results determined using DC in this study are up to 31% lower for Al and 20% lower for Al-Cu than the combined literature data regression fit. Historically, density measurements of metallic liquids do not exhibit much scatter [45]. Despite the accuracy of the viscosity and surface tension measurements, the density results appear to be inconsistent with literature and are cause for concern. Further discussion and analysis will provide a definitive understanding as to why these density results are so low.

2.1 Theoretical and Empirical Models

To further validate the viscosity measurements of oxygen-saturated Al and Al-Cu, the values reported in this study were compared to various theoretical and empirical models. The viscosity of pure liquid Al was calculated using the Arrhenius and Hildebrand equations (paired with empirical parameters determined by Chhabra *et al.* [46]), as well as the Kaptay unified equation and Hirai model. Details of the models are shown in the Appendix.

The Hirai model, presented prior for pure Al, is a very simple calculation that correlates the activation energy with the melting temperature, T_m (K), of the alloy. The model only requires knowledge of the density, molar mass, and melting temperature of the liquid alloy. These variables were obtained from an experimental study conducted by Brillo *et al.* [47] where they employed EML-LD on Al-Cu samples with various compositions.

The viscosity values for pure Al and Al-Cu calculated using the above equations were plotted alongside and compared to measurements using the DC method in Fig. 10 and Fig. 11, respectively. The figures also include the best-fit curve, or regression (with one SE intervals) of the experimental values. The viscosity measurements of Al published in this study are relatively consistent with values calculated using both the Hirai model (0-27% lower) and Kaptay unified equation (13 – 36% lower). At temperatures 1100 K and greater, the values predicted using the Hirai model fall within one SE of the experimental data regression curve. Al-Cu measurements recorded in this work agree to a varying degree with predictions calculated using the Schick, Zang and Hirai models. For experiments conducted at 1029 and 1076 K, results from this study vary by a maximum of 9% from values predicted by Schick and Zhang models. For experiments conducted at 1123, 1180 and 1224 K, the Hirai model predicts values within 22%. All models, with the exception of Moelwyn-Hughes, lie within one SE of the DC results regression at certain points over the fitted temperature range of 1029 – 1224 K. The outcome of this analysis contributes to the merits of the DC technique. Clearly, the data is within reasonable agreements with most theoretical and empirical models, excluding a few which rely on antiquated empirical data, i.e. Chhabra parameters.

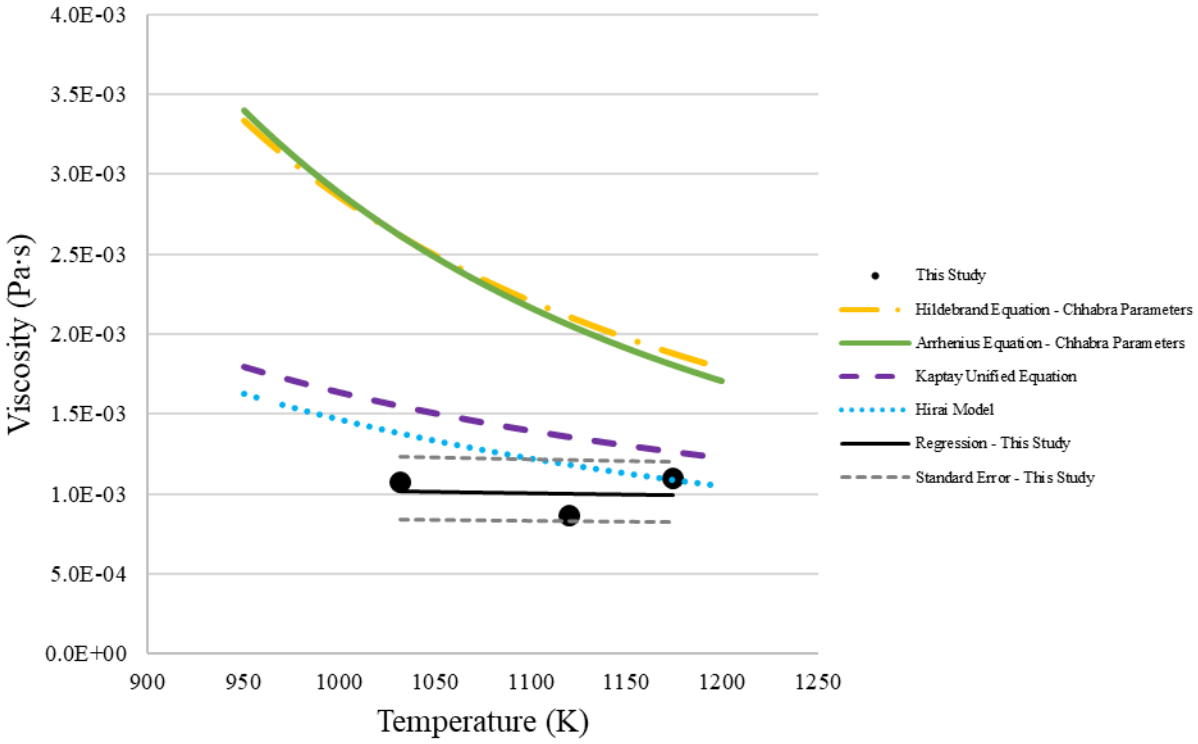

Figure 10: Comparison of Al viscosity measured using the DC method and predictions calculated using theoretical and empirical models

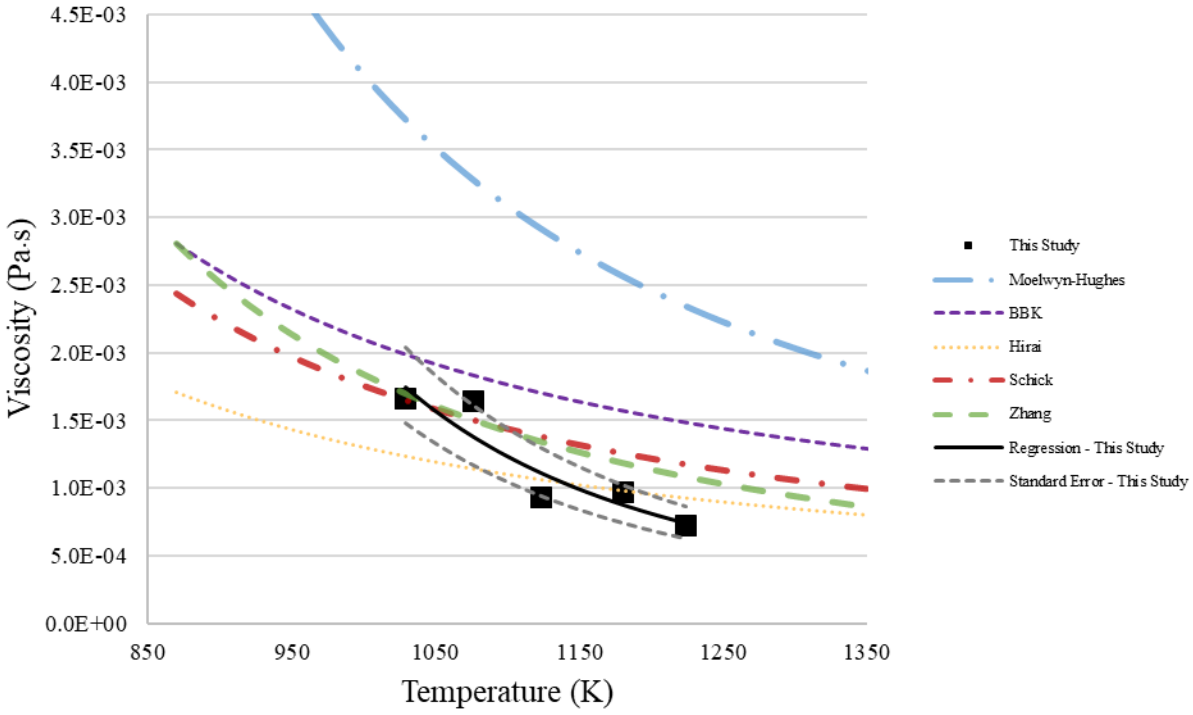

Figure 11: Comparison of Al-Cu viscosity measured using the DC method and predictions calculated using theoretical and empirical models

Much like the analysis conducted for viscosity, as further validation, Al surface tension measured using the DC method was compared to theoretical models . The models selected for this analysis are the Butler model and the Chatain model. Details of the models are presented in the Appendix.

The Butler and Chatain models were previously investigated for the Al-Cu system by Schmitz *et al.* [44], and shown below in Fig. 12 for Al-Cu as a function of temperature. The surface tension results measured using the DC method were also plotted in Fig. 12, along with the regression best-fit model and standard error intervals. The Butler and Chatain models appear to predict the experimental results with high accuracy. Both models were able to predict values within ± 4% of the results reported in this study.

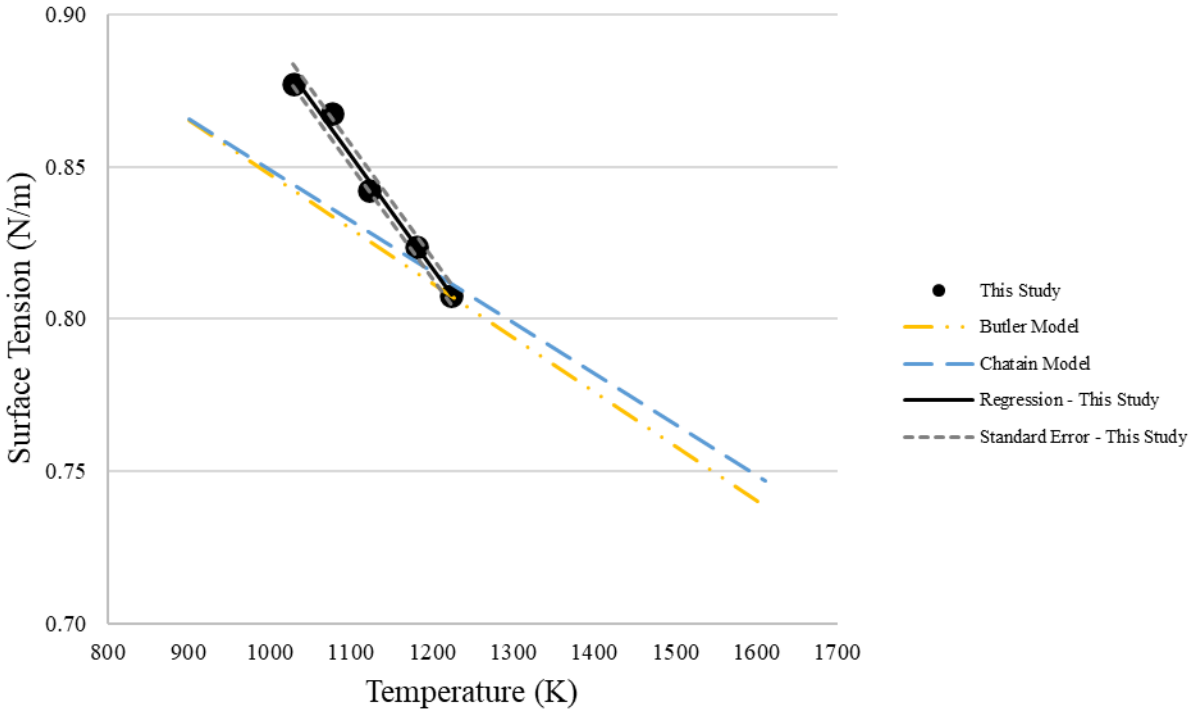

Figure 12: Surface tension data of Al-Cu as a function of temperature from experimental measurements (markers) and theoretical calculations (lines)

2.2 The Effect of Wetting

By comparing viscosity and surface tension measured using the DC method to other results published in literature, as well as values calculated using theoretical models, we are able to say with high certainty that these measurements are reasonably accurate. In stark contrast, density measurements reported in this study were much lower than those reported elsewhere. One possible explanation for inaccurate density results may be linked to the wettability of both Al and Al-Cu on Al_2O_3. If the liquids were to wet the exit of the orifice as the liquid drained, the dynamics of the free jet would be inherently different from what was predicted using the DC model. Previous work using the DC method provided density values in excellent agreement with literature, however, these experiments employed a graphite crucible, as opposed to Al_2O_3. Al and Al-Cu are likely to wet the Al_2O_3 crucible, particularly at the temperatures achieved in this study ($\geq$ 1029 K). Bao *et al.* [48] reported that near melting temperature, Al does not wet Al_2O_3, however, as the temperature rises, wettability increases, exhibiting contact angles below 90 degrees, i.e. $\theta_s < 90°$. Likewise, Klinter *et al.* [49] measured the θ_s between an Al-Cu alloy and Al_2O_3 and noted a similar trend.

Efforts have been made to better understand the effect of wetting on flow rate. In fact, Ferrand [50] considered the effect of wetting on water draining from an orifice under the influence of gravity using bottom plates with different wettability, e.g. glass, PVC, Teflon. They noted that the different bottom plates strongly affected the rate of drainage and observed that "the shape of the meniscus evolves continuously with wettability". They believed that the meniscus either accelerates or decelerates drainage flow depending on its shape and size [50].

The meniscus at the exit of the orifice forms due to capillary action, where adhesion occurs between the Al or Al-Cu and the Al_2O_3 crucible and spreads along the surface until gravitational forces overcome the liquid cohesion. The combination of surface tension (cohesion within the liquid) and the adhesive forces between the liquid and the solid will propel the meniscus outwards. The relationship between wetting of the crucible base and the flow rate of the draining liquid under gravity was further studied using the DC method. This was done by comparing the actual measured flow rate, $Q_{measured}$, (from experiments with liquid Al and Al-Cu) to the expected flow rate, $Q_{literature}$, assuming no wetting occurred; $Q_{literature}$ was calculated applying Eq. 1, but using thermophysical properties published in literature . Recall, the C_d versus Re functions were obtained from water calibrations on crucibles with their bases sprayed with hydrophobic coating. The effect of wetting on flow rate is believed to be correlated to the radius of the growing meniscus which evolves with drain time. Literature has shown that dynamic contact angle, θ_d, formed between a flowing liquid (advancing or receding) and the solid is not constant but reflects the balance between capillary and viscous forces [51]. The relationship between forces is defined by the Capillary number, Ca:

$$Ca = \frac{\eta\left({}^{Q_{theo}}/_{\pi r_o^2}\right)}{\sigma} = \frac{\text{viscous forces}}{\text{surface tension}} \tag{9}$$

Where η is the viscosity of the liquid obtained from published literature. The θ_d is related to small Ca values using Tanner's law [51]:

$$\theta_d \sim Ca^{1/3} \tag{10}$$

In theory, this law is valid over a wide range of Ca, with θ_d decreasing and converging to an equilibrium contact angle as Ca approaches 0 [51]. Simply put, for low Ca values, flow is dominated by capillary or surface tension forces, whereas high Ca values, the capillary forces are negligible compared to viscous forces. A decreasing θ_d fundamentally describes an advancing meniscus front. For both liquid Al and Al-Cu on Al_2O_3, the θ_d decreases with time. By plotting $Q_{measured}/Q_{literature}$ versus Ca (see Fig. 13 for example of Al at 1032 K), we were able to confirm the effect of a growing meniscus, or decreasing θ_d, on the flow, relative to non-wetting conditions.

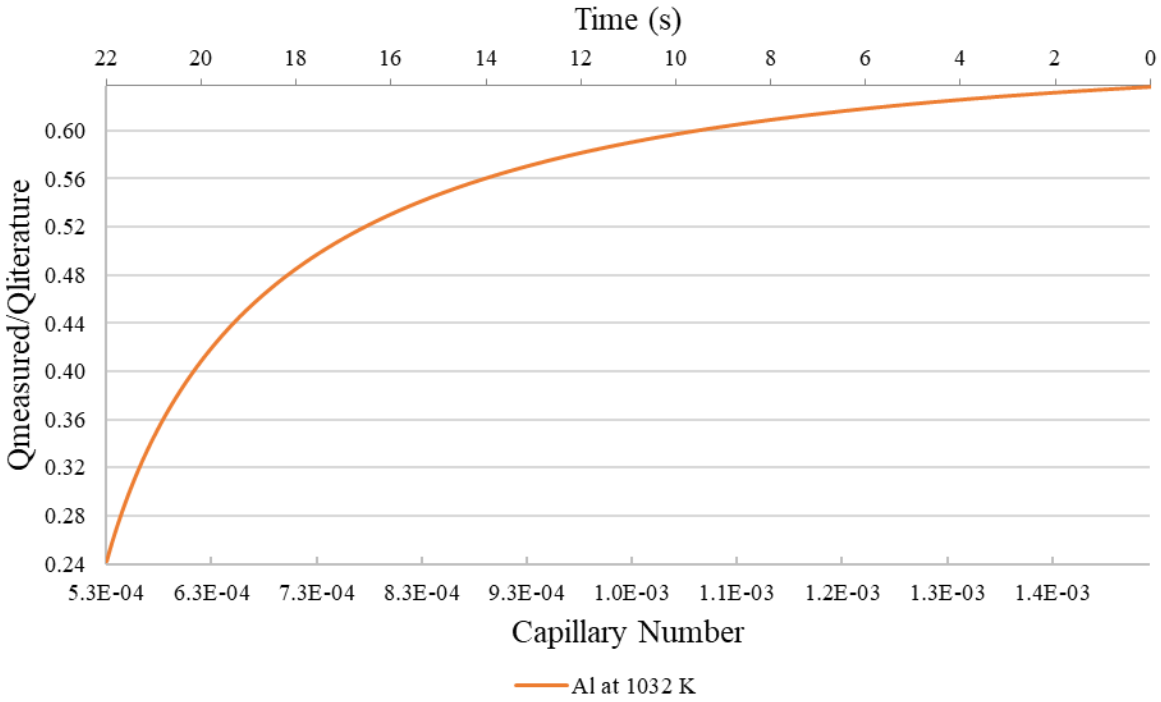

Figure 13: ($Q_{measured}/Q_{literature}$) as a function of Ca for Al at 1032 K

Not only is $Q_{measured}/Q_{literature}$ below 1 giving evidence that wetting reduces flow rate relative to non-wetting conditions, the ratio also appears to decrease with decreasing Ca. Since Ca decreases proportionally with θ_d, Fig. 13 strongly suggests that the lower $Q_{measured}$ of Al (relative to $Q_{literature}$) is related to θ_d, supporting the hypothesis that flow rate is affected by meniscus growth at the outlet of the orifice.

Further evidence of this hypothesis can be observed by examining capillary length, λ_c, which is a length scaling factor that relates gravity forces to surface tension, and is fundamental property that governs the behavior of menisci:

$$\lambda_c = \sqrt{\frac{\sigma}{\rho g}} = \frac{\text{surface tension}}{\text{gravity forces}} \tag{11}$$

Where σ is the gas-liquid surface tension, ρ is the density of the liquid, and g is the gravitational constant. When the radius of the meniscus at the outlet of the orifice is less than λ_c, the shape of the meniscus is governed by surface tension forces, suggesting that the meniscus will continue to grow, up until its radius exceeds λ_c, at which point gravity forces dominate, pulling the edges of the meniscus into the free jet. When calculated for Al at 1032 K, λ_c is equal to 6.10 mm, while the size of the orifice is only 2.65 mm. One would therefore expect the meniscus at the outlet of the orifice to grow more than double in size. By examining these dimensionless numbers, paired with the observations reported by Ferrand [50], we understand that Al and Al-Cu will form a meniscus, which will grow over the course of an experiment, and that due to the reduction in local pressure gradient within the meniscus as it grows, the relative magnitude of flow will be less compared to if drained in non-wetting conditions.

At last, the final question to ask is why does the non-linear least squares regression output provide accurate viscosity and surface tension values (when compared to published data and theoretical models) when density values are so imprecise? In looking at Eq. 3, the algorithm iteratively attempts to determine a set of variables, i.e. surface tension, viscosity, and density, that minimizes the error between measured, h_{exp}, and modelled head, $f(Q_{exp})$. One would expect that all three variables would need to change significantly for the modelled head to line up with its measured counterpart. However, looking at the sensitivity of the model to each respective variables, it is clear that density has the largest impact. This is shown in Fig. 14, where density, surface tension and viscosity of Al at 1032 K were all increased (or decreased) by 25% from the literature values published in Mills [52] and Schmitz *et al.* [44] Assael *et al.* [6], respectively. Fig. 14 reveals that increasing density by 25% has the largest impact on increasing the $f(Q_{exp})$ closer to h_{exp}, compared to when the same percentage is changed for surface tension or viscosity.

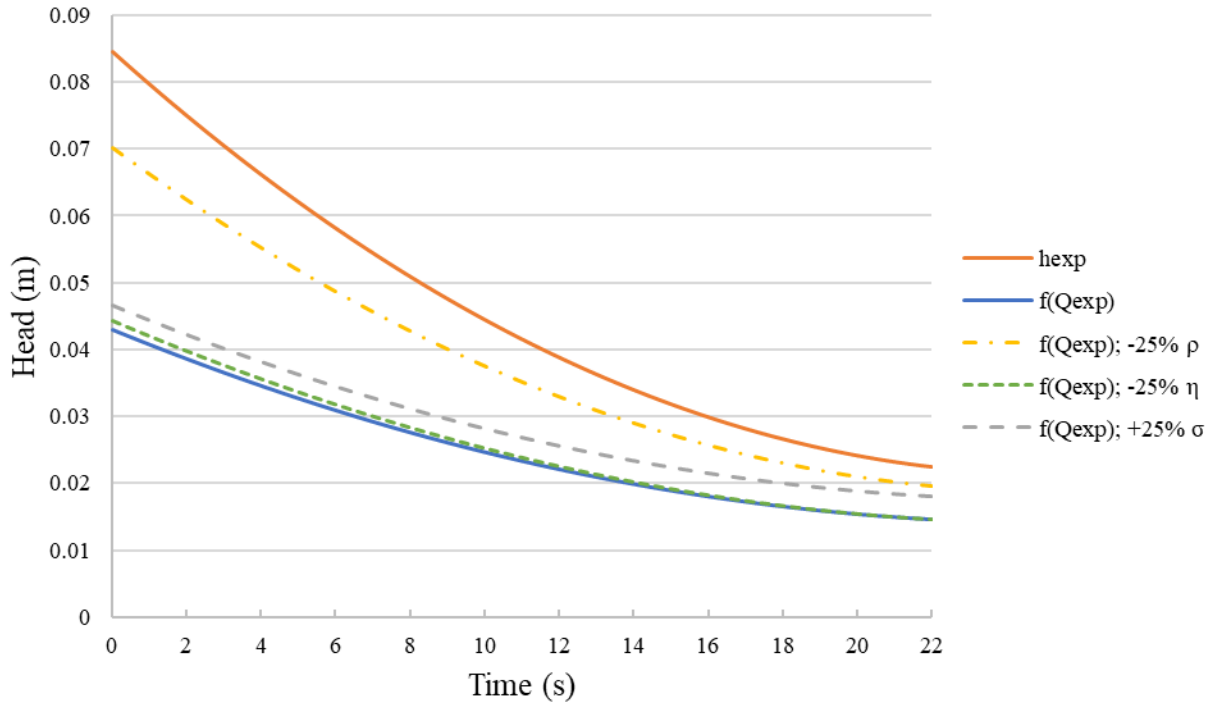

Figure 14: Effect of changing density, surface tension and viscosity by 25% on modelled head

To examine further, the residual sum of squares (RSS) was calculated as a function of density (constant surface tension and viscosity), surface tension (constant density and viscosity) and viscosity (constant density and surface tension) using data from the Al experiment at 1032 K. RSS was calculated by squaring the difference between measured head, $h_{i,exp}$, and modelled head, $f(Q_{i,exp}, \beta)$:

$$RSS = \sum_{i=1}^{m} \left(h_{i,exp} - f(Q_{i,exp}, \beta)\right)^1 \quad (26)$$

To compare against each other, the values were normalized to the same scale by representing the variables in terms of percent change from their converged, or regression, values, which were

reported in Table 1. This is shown in Fig. 15. Here, density has the largest sensitivity or effect in reducing the RSS. For instance, if density were to be updated from -25% of its converged value (iteratively using the Gauss-Newton algorithm), the RSS would be reduced by 0.8. Conversely, for surface tension and viscosity, the RSS would only be reduced by 0.27 and 0.0001, respectively.

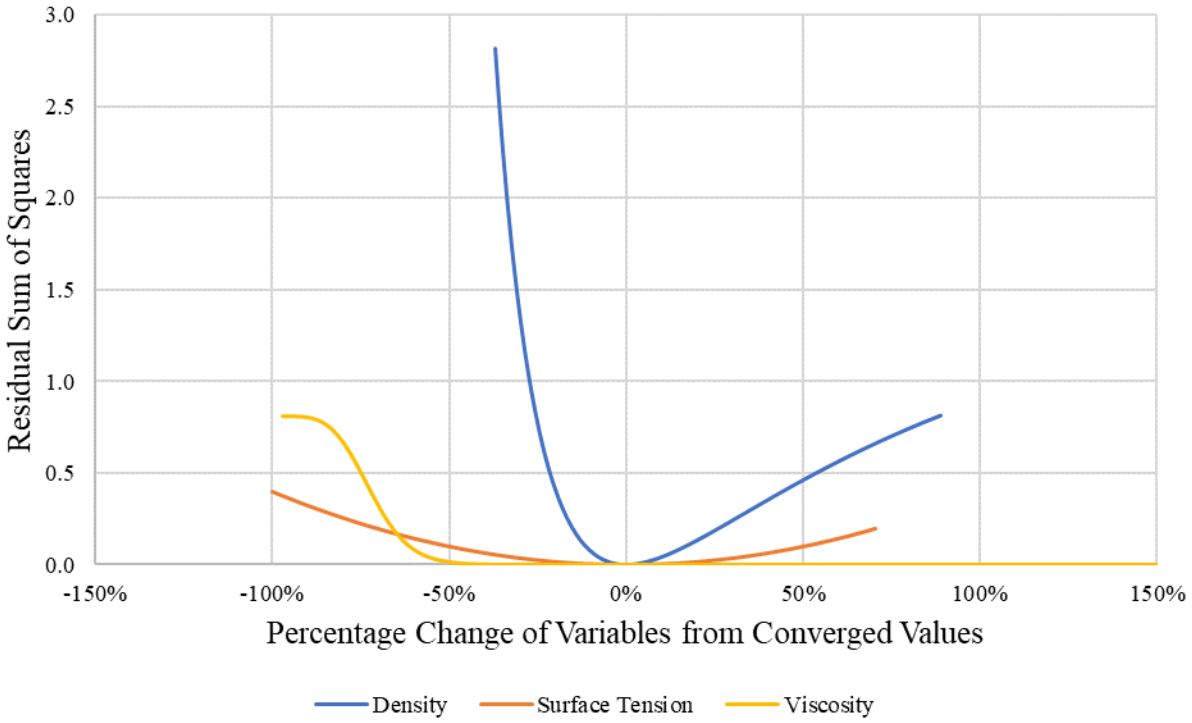

Figure 15: Residual sum of squares of head versus normalized density, surface tension and viscosity

This, in part, explains why the non-linear least squares regression successfully calculated surface tension and viscosity, but not density. For the experimental conditions presented in this work, the model is heavily weighted to changes in density, versus changes in viscosity or surface tension. As such, to minimize error, the algorithm steps in a direction of steepest descent, which as shown above, would be favored in the direction of density.

4. Summary

The viscosity, surface tension and density of 99.9wt.% Al and Al-Cu alloy (consisting of 22.5wt.% Cu) were measured using the DC method with an Al_2O_3 crucible and determined using a multiple nonlinear regression. The flow was modelled based on the Bernoulli formulation, and relates experimental parameters of head and flow rate with viscosity, surface tension and density. Viscous losses were characterized by performing calibration experiments with deionized water to determine a C_d versus Re relationship. Al was measured at 1032, 1120 and 1174 K and Al-Cu at 1029, 1076, 1123, 1180 and 1174 K.

The viscosity and surface tension results for both Al and Al-Cu were in good agreement with comparable results published in literature which were determined using conventional measurement techniques. In contrast, Al and Al-Cu density measurements were in poor agreement

with comparable data published in literature (significantly lower). The largest difference between measured results and the linear regressions obtained from literature data was -31% for Al and -20% for Al-Cu. This is of substantial concern seeing as the spread between density data for both Al and Al-Cu in literature is small.

Ferrand [50] suggested that the meniscus that forms at the exit of the orifice either accelerates or decelerates the flow depending upon its shape. Through analysis, it was determined that the actual measured flow rate of Al and Al-Cu experiments was indeed lower than the expected flow rate predicted by the DC model calculated using thermophysical property values found in literature. It was concluded that the C_d versus Re relationship not only characterizes viscous losses, but also the contribution that wetting has on the flow rate. And, since this relationship was determined using experiments with deionized water and a hydrophobic coated crucible, the calibration function would not translate to high-temperature experiments. This gap ultimately led to the DC model predicting a higher flow rate than measured since it did not account for accelerative losses caused by a growing meniscus. Additionally, analysis revealed that the wetting immediately had an effect on the flow rate of the draining liquid, and the effect became more dominant with increasing drain time. This was supported using dimensionless analysis, where it was determined that the relative difference between measured flow rate and flow rate calculated using the DC model increased as a function of dynamic contact angle, which in turn is related to the Capillary number.

In conclusion, although the DC method (using an Al_2O_3 crucible) was able to successfully measure, despite wetting at the orifice tip, the viscosity and surface tension of both O saturated Al and an Al-Cu alloy at various temperatures, it was not capable of accurately measuring density. This is due to the fact that for the experimental conditions presented in this study, the DC model using to predict flow rate (or tangentially head) was weighted more towards density, versus surface tension or viscosity. Thus, lowering density had the largest effect due to orifice wetting, on minimizing the sum of squares of the residuals, and hence achieving regression convergence. Future research is aimed at extending the DC model and method to account for fluid wetting at the orifice.

References

[1] H. Kvande, "The Aluminum Smelting Process," *J. Occup. Environ. Med.*, vol. 56, no. 5, pp. 2–4, 2014.

[2] I. F. Bainbridge and J. A. Taylor, "The Surface Tension of Pure Aluminum and Aluminum Alloys," *Metall. Mater. Trans. A*, vol. 44, no. 8, pp. 3901–3909, 2013.

[3] M. Schick, J. Brillo, I. Egry, and B. Hallstedt, "Viscosity of Al-Cu liquid alloys: measurement and thermodynamic description," *J. Mater. Sci.*, vol. 47, no. 23, pp. 8145–8152, 2012.

[4] J. J. Wessing and J. Brillo, "Density, Molar Volume, and Surface Tension of Liquid Al-Ti," *Metall. Mater. Trans. A*, vol. 48, no. 2, pp. 868–882, 2017.

[5] E. Louvis, P. Fox, and C. J. Sutcliffe, "Selective laser melting of aluminium components," *J. Mater. Process. Tech.*, vol. 211, no. 2, pp. 275–284, 2011.

[6] M. J. Assael *et al.*, "Reference Data for the Density and Viscosity of Liquid Aluminum and Liquid Iron," *J. Phys. Chem. Ref. Data*, vol. 35, no. 1, pp. 285–300, 2006.

[7] S. J. Roach and H. Henein, “A New Method to Dynamically Measure the Surface Tension, Viscosity, and Density of Melts,” *Metall. Mater. Trans. B*, vol. 36, no. 5, pp. 667–676, 2005.
[8] S. Roach and H. Henein, “A Dynamic Approach to Determining the Surface Tension of a Fluid,” *Can. Metall. Q.*, vol. 42, no. 2, pp. 175–186, 2003.
[9] T. Gancarz, J. Jourdan, W. Gasior, and H. Henein, “Physicochemical properties of Al, Al-Mg and Al-Mg-Zn alloys,” *J. Mol. Liq.*, vol. 249, pp. 470–476, 2018.
[10] T. Gancarz and W. Gasior, “Density, Surface Tension, and Viscosity of Liquid Pb-Sb Alloys,” *J. Chem. Eng. Data*, vol. 63, no. 5, pp. 1471–1479, 2018.
[11] T. Gancarz, W. Gąsior, and H. Henein, “The Discharge Crucible Method for Making Measurements of the Physical Properties of Melts: An Overview,” *Int J Thermophys*, vol. 35, no. 9–10, pp. 1725–1748, 2014.
[12] T. Gancarz, W. Gąsior, and H. Henein, “Physicochemical Properties of Sb, Sn, Zn, and Sb-Sn System,” *Int. J. Thermophys.*, vol. 34, no. 2, pp. 250–266, 2013.
[13] T. Gancarz, “Physicochemical Properties of Sb-Sn-Zn Alloys,” *J. Electron. Mater.*, vol. 43, no. 12, pp. 4374–4385, 2014.
[14] T. Gancarz, “Density, surface tension and viscosity of Ga-Sn alloys,” *J. Mol. Liq.*, vol. 241, pp. 231–236, 2017.
[15] T. Gancarz, “Density, surface tension and viscosity of liquid ZnAl + X (X = Li, Na, Si) alloys,” *Fluid Phase Equilib.*, vol. 427, pp. 97–103, 2016.
[16] Y. Plevachuk, V. Sklyarchuk, A. Yakymovych, S. Eckert, B. Willers, and K. Eigenfeld, “Density, Viscosity, and Electrical Conductivity of Hypoeutectic Al-Cu Liquid Alloys,” *Metall. Mater. Trans. A*, vol. 39, no. 12, pp. 3040–3045, 2008.
[17] W. Jones and W. Bartlett, “The Viscosity of Aluminum and Binary Aluminum Alloys,” *J. Inst. Met.*, vol. 81, no. 3, pp. 145–152, 1952.
[18] T. P. Yao and V. Kondic, “The viscosity of molten tin, lead, zinc, aluminium, and some of their alloys,” *J. Inst. Met.*, vol. 81, pp. 17–24, 1952.
[19] T. Yamasaki, S. Kanatani, Y. Ogino, and A. Inoue, “Viscosity measurements for liquid Al-Ni-La and Al-Ni-Mm (Mm: Mischmetal) alloys by an oscillating crucible method,” *J. Non. Cryst. Solids*, vol. 156–158, pp. 441–444, 1993.
[20] H. A. Friedrichs, L. W. Ronkow, and Y. Zhou, “Measurement of viscosity, density and surface tension of metal melts,” *Steel Res.*, vol. 68, no. 5, pp. 209–214, 1997.
[21] R. J. L. Andon, L. A. Chapman, A. P. Day, and K. C. Mills, “Viscosities of liquid metals and commercial alloys,” Middlesex, UK, 1999.
[22] D. Wang and R. A. Overfelt, “Oscillating Cup Viscosity Measurements of Aluminum Alloys: A201, A319 and A356,” *Int. J. Thermophys.*, vol. 23, no. 4, pp. 1063–1076, 2002.
[23] S. H. Park, Y. S. Um, C. H. Kum, and B. Y. Hur, “Thermophysical properties of Al and Mg alloys for metal foam fabrication,” *Colloids Surfaces A Physicochem. Eng. Asp.*, vol. 263, no. 1–3, pp. 280–283, 2005.
[24] H. Kobatake, J. Schmitz, and J. Brillo, “Density and viscosity of ternary Al-Cu-Si liquid alloys,” *J. Mater. Sci.*, vol. 49, no. 9, pp. 3541–3549, 2014.
[25] N. Eustathopoulos, J. C. Joud, P. Desre, and J. M. Hicter, “The wetting of carbon by aluminium and aluminium alloys,” *J. Mater. Sci.*, vol. 9, no. 8, pp. 1233–1242, 1974.
[26] P. Laty, J. C. Joud, P. Desré, and G. Lang, “Tension superficielle d’alliages liquid aluminum-cuivre,” *Surf. Sci.*, vol. 69, no. 2, pp. 508–520, 1977.
[27] J. Schmitz, J. Brillo, and I. Egry, “Surface tension of liquid Al-Cu and wetting at the Cu/Sapphire solid-liquid interface,” *Eur. Phys. J. Spec. Top.*, vol. 223, no. 3, pp. 469–479,

2014.
[28] J. M. Molina, R. Voytovych, E. Louis, and N. Eustathopoulos, “The surface tension of liquid aluminium in high vacuum: The role of surface condition,” *Int. J. Adhes. Adhes.*, vol. 27, no. 5, pp. 394–401, 2007.
[29] W. D. Drotning, “Thermal expansion and density measurements of molten and solid materials at high temperatures by the gamma attenuation technique,” Sandia National Laboratories, Albuquerque, NM, USA, 1979.
[30] P. M. Nasch and S. G. Steinemann, “Density and thermal expansion of molten manganese, iron, nickel, copper, aluminum and tin by means of the gamma-ray attenuation technique,” *Phys. Chem. Liq.*, vol. 29, no. 1, pp. 43–58, 1995.
[31] P. M. Smith, J. W. Elmer, and G. F. Gallegos, “Measurement of the density of liquid aluminum alloys by an X-ray attenuation technique,” *Scr. Mater.*, vol. 40, no. 8, pp. 937–941, 1999.
[32] V. Sarou-Kanian, F. Millot, and J. C. Rifflet, “Surface Tension and Density of Oxygen-Free Liquid Aluminum at High Temperature,” *Int. J. Thermophys.*, vol. 24, no. 1, pp. 277–286, 2003.
[33] H. L. Peng, T. Voigtmann, G. Kolland, H. Kobatake, and J. Brillo, “Structural and dynamical properties of liquid Al-Au alloys,” vol. 184201, pp. 1–13, 2015.
[34] M. Leitner, T. Leitner, A. Schmon, K. Aziz, and G. Pottlacher, “Thermophysical Properties of Liquid Aluminum,” *Metall. Mater. Trans. A*, vol. 48, no. 6, pp. 3036–3045, 2017.
[35] N. Y. Konstantinova, P. S. Popel’, and D. A. Yagodin, “The kinematic viscosity of liquid copper-aluminum alloys,” *High Temp.*, vol. 47, no. 3, pp. 336–341, 2009.
[36] K. C. Mills and Y. C. Su, “Review of surface tension data for metallic elements and alloys: Part 1 – Pure metals,” *Int. Mater. Rev.*, vol. 51, no. 6, pp. 329–351, 2006.
[37] A. Pamies, C. Garcia-Cordovilla, and E. Louis, “The measurement of surface tension of liquid aluminum by means of the maximum bubble pressure method: the effect of surface oxidation,” *Scr. Metall.*, vol. 18, no. 9, pp. 869–872, 1984.
[38] J. P. Anson, R. A. L. Drew, and J. E. Gruzleski, “The Surface Tension of Molten Aluminum and Al-Si-Mg Alloy under Vacuum and Hydrogen Atmospheres,” *Metall. Mater. Trans. B*, vol. 30, no. 6, pp. 1027–1032, 1999.
[39] Y. Wang, Y. Wu, and X. Bian, “Composition dependence of viscosity for Al(1-x)Mgx(0≤x≤0.10) alloys,” *Chinese Sci. Bull.*, vol. 52, no. 11, pp. 1441–1445, 2007.
[40] R. F. Brooks, A. T. Dinsdale, and P. N. Quested, “The measurement of viscosity of alloys—a review of methods, data and models,” *Meas. Sci. Technol.*, vol. 16, no. 2, pp. 354–362, 2005.
[41] N. Jakse and A. Pasturel, “Liquid Aluminum: Atomic diffusion and viscosity from ab initio molecular dynamics,” *Sci. Rep.*, vol. 3, no. 1, pp. 1–8, 2013.
[42] C. Garcia-Cordovilla, E. Louis, and A. Pamies, “The surface tension of liquid pure aluminium and aluminium-magnesium alloy,” *J. Mater. Sci.*, vol. 21, no. 8, pp. 2787–2792, 1986.
[43] L. Goumiri, J. C. Joud, and P. Desre, “Tensions superficielles d’alliages liquides binaires présentant un caractère dimmiscibilité: Al-Pb, Al-Bi, Al-Sn et Zn-Bi,” *Surf. Sci.*, vol. 83, no. 2, pp. 471–486, 1979.
[44] J. Schmitz, J. Brillo, I. Egry, and R. Schmid-Fetzer, “Surface tension of liquid Al–Cu binary alloys,” *Int. J. Mater. Res.*, vol. 100, no. 11, pp. 1529–1535, 2009.
[45] T. Iida and R. I. L. Guthrie, *The Thermophysical Properties of Metallic Liquids*, 1st ed.

Oxford, UK: Oxford University Press, 2015.
[46] R. P. Chhabra and D. K. Sheth, "Viscosity of molten metals and its temperature dependence," *Zeitschrift fur Met.*, vol. 81, no. 4, pp. 264–271, 1990.
[47] J. Brillo, I. Egry, and I. Ho, "Density and thermal expansion of liquid Al–Ag and Al–Cu alloys," *Int. J. Mater. Res.*, vol. 99, no. 2, pp. 162–167, 2008.
[48] S. Bao, K. Tang, A. Kvithyld, M. Tangstad, and T. A. Engh, "Wettability of aluminum on alumina," *Metall. Mater. Trans. B*, vol. 42, no. 6, pp. 1358–1366, Dec. 2011.
[49] A. J. Klinter, G. Mendoza-Suarez, and R. A. L. Drew, "Wetting of pure aluminum and selected alloys on polycrystalline alumina and sapphire," *Mater. Sci. Eng. A*, vol. 495, no. 1–2, pp. 147–152, 2008.
[50] J. Ferrand, "Écoulements et écrasements de fluides: effet du mouillage et de la rhéologie," Ph.D. dissertation, École Doctorale de Physique et d'Astrophysique de Lyon, l'École Normale Supérieure de Lyon, Lyon, France, 2017.
[51] J. Berthier, *Micro-Drops and Digital Microfluidics*, 2nd ed. Oxford, UK: William Andrew, 2012.
[52] K. C. Mills, *Recommended values of thermophysical properties for selected commercial alloys*. Cambridge, UK: Woodhead Publishing Limited, 2002.
[53] J. H. Hildebrand, *Viscosity and Diffusivity: A Predictive Treatment*. John Wiley & Sons, 1977.
[54] G. Kaptay, "A unified equation for the viscosity of pure liquid metals," *Zeitschrift für Met.*, vol. 96, no. 1, pp. 24–31, 2005.
[55] M. Hirai, "Estimation of viscosities of liquid alloys," *ISIJ Int.*, vol. 33, no. 2, pp. 251–258, 1993.
[56] E. A. Moelwyn-Hughes, *Physical Chemistry*, 2nd ed. New York, NY, USA: Pergamon Press, 1961.
[57] D. S. Kanibolotsky, O. A. Bieloborodova, and N. V. Kotova, "Thermodynamic properties of liquid Al-Si and Al-Cu alloys," *J. Therm. Anal. Calorim.*, vol. 70, no. 3, pp. 975–983, 2002.
[58] I. Budai, M. Z. Benkő, and G. Kaptay, "Comparison of Different Theoretical Models to Experimental Data on Viscosity of Binary Liquid Alloys," *Mater. Sci. Forum*, vol. 537–538, pp. 489–496, 2007.
[59] J. Brillo, *Thermophysical Properties of Multicomponent Liquid Alloys*. Berlin, Germany: Walter de Gruyter GmbH & Co KG, 2016.
[60] F. Zhang, Y. Du, S. Liu, and W. Jie, "Modeling of the viscosity in the AL-Cu-Mg-Si system: Database construction," *Calphad Comput. Coupling Phase Diagrams Thermochem.*, vol. 49, pp. 79–86, 2015.
[61] J. A. V. Butler, "The Thermodynamics of the Surfaces of Solutions," *Proc. R. Soc. London. Ser. A, Contain. Pap. a Math. Phys. Character*, vol. 135, no. 827, pp. 348–375, 1932.
[62] J. Brillo, D. Chatain, and I. Egry, "Surface tension of liquid binary alloys – theory versus experiment," *Int. J. Mater. Res.*, vol. 100, no. 1, pp. 53–58, 2009.

Appendix A

A.1 Viscosity of Al

A.1.1 The Arrhenius Model

The Arrhenius equation is the most commonly used model to describe the temperature dependence of the viscosity of pure metals, and has also been used to describe the viscosities of some liquid alloys [45]:

$$\eta = \eta_\infty \exp\left(\frac{E_a}{RT}\right) \quad \text{(A1)}$$

Where E_a is the activation energy for viscous flow (J/mol), R is the gas constant (8.3144 J mol^{-1} K^{-1}), T is the temperature (K), and η_∞ is the pre-exponential factor (Pa·s). Chhabra *et al.* [46] determined that E_a, and η_∞ for pure liquid Al were 26.12 kJ and 0.1245 mPa·s, respectively.

A.1.2 The Hildebrand Model

Hildebrand [53] developed an equation for the viscosity of liquids based on the principle that fluid flow is governed by the free space available. He reasoned that fluidity, $\phi = 1/\eta$ (1/Pa·s), should decrease with decreasing temperature, due to molecules becoming more closely packed. The fluidity should decrease to a point where they would be too crowded to permit free flow, and ϕ becomes zero. As such, he defined an equation describing the fluidity of a liquid:

$$\phi = \frac{1}{\eta} = B\left(\frac{V_M - V_0}{V_0}\right) \quad \text{(A2)}$$

Where V_0 (m^3/mol) is the intrinsic volume where flow is stopped, V_M (m^3/mol) is the molar volume and B (1/Pa·s) is a characteristic constant. Both V_0 and B are constants independent of temperature, and Chhabra *et al.* [46] derived these constants for pure Al as 10.76 cm^3/mol and 5.719, respectively.

A.1.3 The Kaptay Model

Kaptay [54] presented a unified equation, using premises from both the activation energy and the free volume theories:

$$\eta = A_K \frac{M^{1/2}}{V_m^{2/3}} \exp\left(B_K \frac{T_m}{T}\right) \quad \text{(A3)}$$

Where A_K and B_K are constants. The equation was tested on 15 liquid metals (101 individual measurements), and the average values for the constants A_K and B_K were found to be (1.80 ± 0.39) x 10^{-8} (J/Kmol$^{1/3}$)$^{1/2}$ and 2.34 ± 0.20, respectively.

A.1.4 The Hirai Model

Hirai [55] developed a simple relationship for E_a (J/mol) by plotting the $\ln \eta$ vs $\frac{1}{T}$ (K^{-1}) for various pure metals and alloys which yields a slope of $\frac{E_a}{R}$ (K^{-1}):

$$E_a = 2.65 T_m^{1.27} \text{ (J mol}^{-1}\text{)} \quad \text{(A4)}$$

Hirai also suggested a way of combining both the Andrade equation (i.e. $\eta_m = C_A T_m^{1/2} \rho_m^{2/3} M^{-1/6}$) and Arrhenius equation to express an equation for η_∞ (Pa·s):

$$\eta_\infty = \frac{1.7\ x\ 10^{-7}\ \rho^{2/3} T_m^{1/2} M^{-1/6}}{\exp(2.65 T_m^{0.27}/R)} \quad \text{(A5)}$$

A.2 Viscosity of Al-Cu alloy

The viscosity of liquid Al-Cu reported in this study was compared to predicted values calculated using the Hirai model, the Moelwyn-Hughes model, the BBK model, the Schick model, and the Zhang model.

A.2.1 Moelwyn-Hughes Model

Moelwyn-Hughes [56] proposed that the viscosities of binary liquid mixtures be described by:

$$\eta = (x_A \eta_A + x_B \eta_B)\left(1 - 2x_A x_B \frac{\Delta u}{\kappa T}\right) \quad \text{(A6)}$$

Where η_A and η_B are the viscosities of the pure liquid metals (Pa·s), x_A and x_B are the mole fractions of the pure liquid metals, κ is the Boltzmann constant and $\Delta u = \Delta H / x_A x_B N_A$; ΔH is the (integral) enthalpy of mixing (J/mol) and N_A is Avogadro's constant (mol^{-1}). The enthalpy of mixing was calculated using an equation proposed by Kanibolotsky *et al.* [57] based on direct calorimetric data:

$$\Delta H = x_{Cu}(1 - x_{Cu})(-37.72 - 18.45 x_{Cu} - 60.67 x_{Cu}^2) \quad \text{(kJ/mol)} \quad \text{(A7)}$$

A.2.2 The BBK Model

Unlike the Moelwyn-Hughes model, Budai, Bemko and Kaptay (BBK) [58] derived a new equation capable of calculating the viscosities of any multicomponent liquid metal system even when the viscosities of the pure liquid metals are unknown:

$$\eta = A \frac{(\sum x_i M_i)^{1/2}}{\left(\sum x_i V_{m,i} + \Delta V^E\right)^{2/3}} T^{1/2} \exp\left[\frac{B}{T}\left(\sum x_i T_{m,i} - \frac{\Delta H}{qR}\right)\right] \quad \text{(A8)}$$

Where A and B are the same constants as in the Kaptay unified model, q is a semi-empirical parameter ($q \approx 24.4 \pm 2$), ΔV^E is the excess molar volume upon alloy formation (m^3/mol) which can be taken as zero when experimental data are not available.

A.2.3 The Schick Model

Schick [59] attempted to account for the effect of strong interactions between atoms on the viscosity of liquid metallic binary systems. The model, based on the Arrhenius equation, assumes that the activation energy, E_a (J/mol), is generally larger if unlike atoms are more attracted to each other. Hence, E_a can be expressed as a function of the enthalpy of mixing, ΔH (J/mol):

$$E_a = \sum x_i E_{a,i} - \Delta H + RT \sum x_i \ln x_i \quad \text{(A9)}$$

And the pre-exponential factor, η_∞ (Pa·s) is calculated from the following relationship:

$$\ln \eta_\infty = \sum x_i \ln \eta_i \tag{A10}$$

Where η_i is the viscosity of the pure components. $E_{a,i}$ and η_i for the pure components Al and Cu were measured by Schick *et al.* [3]

A.2.4 The Zhang Model

Finally, Zhang *et al.* [60] attempted to specifically consider the effects of "associates", i.e. clustering, in the liquid phase. They proposed a model that can be expressed in two parts: one for ideal mixing and other for the excess viscosity (using the Redlich-Kister polynomial):

$$\eta = \sum_{i=1}^{m} x_i \eta_i + \sum_i \sum_{j>i} x_i x_j \sum A^k \left(x_i - x_j\right)^k \tag{A11}$$

Where A^k (mPa·s) is determined experimentally; A_k used to calculate the viscosity of liquid Al-Cu was provided by Zhang *et al.* [60]

A.3 Surface tension

A.3.1 The Butler Model

The Butler model was one of the first analytical models for the prediction of surface tension [61] . It is based on the supposition that the phase between the bulk liquid and gas phases is considered a separate thermodynamic phase consisting of a monolayer of atoms, which is in equilibrium with the bulk phase. The gas phase is ignored. For a binary alloy, or sub-regular solution, consisting of elements A and B, with corresponding surface tensions, σ_i $(i = A, B)$ (N/m), the surface tension, σ (N/m), of the system can be predicted using the following equation [62]:

$$\sigma = \sigma_i + \frac{RT}{A_i} \ln\left(\frac{c_i^S}{c_i^B}\right) + \frac{1}{A_i}\left({}^E G_i^S\left(T, c_i^S\right) - {}^E G_i^B\left(T, c_i^B\right)\right) \tag{A12}$$

Where R is the universal gas constant (J/mol·K), T is the temperature (K), c_i^B is the mole fraction of component i in the bulk phase, c_i^S is the mole fraction of component i in the surface phase, ${}^E G_i^B$ is the partial excess Gibbs energy in the bulk (J/mol), ${}^E G_i^S$ is the partial excess Gibbs energy of component i in the surface layer (J/mol), and A_i is the surface area in the monolayer of one mole of pure liquid substance (m^2/mol).

A.3.2 The Chatain Model

The Butler model has been heavily criticized as it is closer to a semi-empirical model than an analytical model. Some reasons for this criticism include: the factor β is arbitrary, the mono-layer assumption does not reflect reality in most systems, and the Butler model disagrees with the Gibb-adsorption isotherm. Thus, the Chatain model, or the multilayer model, was developed to remedy these issues, and rather than considering a sole monolayer as the surface, it considers a stack of atomic layers, each with different compositions. The surface tension of liquid binary alloys, consisting of elements A and B, can be calculated using the following expression [62]:

$$A \cdot \sigma = c_A^{(1)} \cdot \varphi_{AA} + c_B^S \cdot \varphi_{BB} - z_v\omega \cdot \left(c_B^{(1)} - 2c_B^B c_B^{(1)} + c_B^{B^2}\right) - 2z_v\omega \cdot \sum_{j=1}^{k} \left(c_B^{(j)} - c_B^B\right)\left(c_B^{(j+1)} - c_B^B\right) - z_1\omega \cdot \sum_{j=1}^{k} \left(c_B^{(j)} - c_B^B\right)^2 + RT \cdot \sum_{j=1}^{k} \left(c_B^{(j)} \cdot \ln\left(\frac{c_B^{(j)}}{c_B^B}\right) + c_A^{(j)} \cdot \ln\left(\frac{c_A^{(j)}}{c_A^B}\right)\right) \quad \text{(A13)}$$

Where $c_A^{(i)} = 1 - c_B^{(i)}$ and $c_A^{(B)} = 1 - c_B^{(B)}$ are the atom fractions of components A and B in the jth layer, and in the bulk (i.e. $c_A^{(j>k)} = c_A^{(B)}$, where k is selected such that the composition of the $(k+1)th$ layer is the same composition as the bulk), respectively, φ_{ij} (with $i, j = A, B$) is the nearest neighbor bond energies (J/mol), z_v is the number of neighbors of an atom in an adjacent layer, and z_1 is the number of neighbors in any given atom layer parallel to the surface. The atoms of the liquid are assumed to reside in lattice sites with a coordination number of $z = 12$, therefore, z_v=3 and $z_1 = 6$ [62]. The parameter ω (J/mol) characterizes the interaction between the components A and B, and is defined by:

$$\omega = \varphi_{AB} - [\varphi_{AA} + \varphi_{BB}]/2 \quad \text{(A14)}$$

To apply the multilayer model, the surface tension is solved using a Monte-Carlo algorithm with random sampling [62].